Synthesize Analysis of the IFN-γ and Immune Infiltrates of m6A RNA Methylation Regulators in Human Skin Cutaneous Melanoma

Yuqi Wang
Jilin Normal University
Le Huang
Jilin Normal University
Mingxin Li
Jilin Normal University
Yunfeng Qi (13500966718@qq.com)
https://orcid.org/0000-0002-2704-6792

Research

Keywords: Skin cutaneous melanoma, N6-methyl adenosine, IFN-γ, cluster analysis, prognosis

Posted Date: October 14th, 2021

DOI: https://doi.org/10.21203/rs.3.rs-919313/v1

Abstract

Background: SKCM is a major common cancer with highly mortality and morbidity, causing about 72% of deaths in skin carcinoma. In recent years, more scholars have selected one or two m^6A regulatory factors to explore the abnormal expression and potential mechanism of m^6A in tumorigenesis and development. So as to find the relevant biomarkers in the whole tumorigenesis process.

Methods: In current study, we used public transcriptome datasets from The Cancer Genome Atlas (TCGA), Gene Expression Omnibus (GEO) and Genotype-Tissue Expression (GTEx) to investigate the relationships between N^6-methyl adenosine(m^6A) regulators genes and Skin cutaneous melanoma (SKCM). Then, SKCM patients were grouped based on the cluster analysis of m^6A regulators expression. Compared the relationship between Interferon (IFN)-γ and immune infiltrates.

Results: Based on the survival curves of subgroups, we selected 20 potential predictive m^6A-related genes were overexpressed in SKCM. And based on the typing results, we got the 15 differential expression genes between the three groups. Four of them (*CYP2U1, SEMA6A, GRIA2*, and *TSPAN13*) were selected in Cox regression, which were significant expression in overall survival($p<0.05$). Interferon (IFN)-γ is a central cytokine, which effecting immune-provoking and recognizing transformed cells in anti-tumour immunity.

Conclusions: To investigate the correlation between IFN-γ and SKCM. We have identified that IFN-γ is a potential factor for cancer therapy, and affecting expression pathways of SKCM. Among them, IFN-γ and *WTAP* were the most positive correlation. These sights suggest that IFN-γ can potentially be utilized for immune pathway such as melanoma skin cancer.

Background

Skin cutaneous melanoma (SKCM) is considered a dangerous cancer with high prevalence and complicated malignancies[1]. The incidence of malignant melanoma accounts for only approximately 5% of skin malignant tumors, but the morbidity and mortality of melanoma have increased to 75% in 2018[2]. Despite the implement to public health campaigns in clinical treatment, the death rates of SKCM are still rising in many counties. What makes it terrible is no effective systematic therapy for SKCM recently. Melanoma has a high potential for metastasis and the prognosis for advanced forms was catastrophically. In clinical trial, surgery remains the reference treatment at the local stage[3]. In prior studies, SKCM has been treated with four new approvals in the adjuvant setting, including nivolumab (for all comers), ipilimumab, dabrafenib and trametinib (for patients with *BARF*-mutated melanoma)[4]. The overall survival (OS) for melanoma is improving equally rapidly[5]. But the overall disease control rates and treatment strategies remain to be improved with fewer patients benefiting from immunotherapy. Targeted therapies and immune-modulatory therapies have changed median survival for melanoma in clinical trials[6]. Immunotherapy and clinicopathological features have been studied and are reviewed extensively by. However, the correlation and factors of immune regulators and SKCM are yet to be fully elucidated. Thus, the regulatory mechanism of tumour immune microenvironment (TIME) should be further explored to determine treatment factors and effective biomarkers. N^6-methyladenosine (m^6A) is a prevalent post and internal transcriptional modification in the N^6-position of adenosine, which is the methylation modification at the sixth N atom of adenine[7, 8]. The m^6A regulators has emerged as an important role of a variety of tumor progression and biological pathway, attracting accumulating attention in bioscience processes[9]. Accumulating evidence suggests that alteration of m^6A levels participates in cancer pathogenesis and development via regulating expression of tumour-related genes (TRGs) like *BRD4*, *MYC*, *SOCS2* and *EGFR*[10]. M^6A modification of mRNAs is mediated by an mRNA-modifying complex, this structural diversity provides more regulatory potential to sort groups of RNAs for affected gene expressive metabolism and functions[11]. The m^6A methylation is highly correlated with expression of intracellular methyltransferases(“writers”) that install methylation, demethylases(“erasers”) that alter the modification level, and binding proteins(“readers”) that recognize the chemical marks[12]. Manifestation of these effector proteins have emphasised multifaceted and controllable features of their functions in sundry biological processes. The “Writers,” which include Methyltransferase Like 3 (*METTL3*)[13], *METTL14*[14–16], Wilms Tumour 1 Associated Protein (*WTAP*)[17–19], *VIRMA*[20], RNA Binding Motif Protein 15 (*RBM15*)[21], and zinc finger CCCH domain-containing protein 13 (*ZC3H13*)[22] as a multicomponent methyltransferase complex of m^6A. The “Erasers,” which comprise fat mass and obesity-associated protein (*FTO*) and α-ketoglutarate-dependent dioxygenase AlkB homolog 5 (*ALKBH5*)[23, 24], have demethylase activity of reversible post-transcriptional modification in mRNAs and the methylation-dependent processes can be reversed. The “Readers,” which cover YTH domain-containing 1 (*YTHDC1*)[25], *YTHDC2*, *YTHN6*-methyl-adenosine RNA-binding protein 1 (*YTHDF1*), *YTHDF2, YTHDF3*, heterogeneous nuclear ribonucleoprotein C (*HNRNPC*), can recognize m^6A modification and decay of their common mRNA targets in cytosol[26]. Recent studies on multi-omics analysis, more scholars choose one or two of m^6A regulators to explore its aberrant expression and underlying mechanism in occurrence and progression of tumours[27]. Li et al. showed that these m^6A-related regulators are frequently dysregulated and correlate with metastasis in Osteosarcoma. *HNRNPA2B1* might be an independent risk factor as novel therapeutic targets and prognostic biomarkers for Osteosarcoma [28]. Han et al. suggested that *METTL3* may interact with the microprocessor protein DGCR8 to cause the process of cancer[29]. Wang et al. suggested that m^6A RNA methylation greatly impacts RNA metabolism and is involved in the pathogenesis of cancer[30]. In addition, Wang et al. proposed that m^6Ascore was based on the expression of immune cell infiltration as modulators. Patients with higher resting CD4 + T infiltration in SKCM[31]. Recent studies have deeply probe into immunotherapy of m^6A regulators with IFN-γ, although its precise molecular mechanism remains unclear.

As we known, exploration of IFN-γ with immune conditions may shed new light on the diagnosis, development, and the immune treatment of SKCM[32]. However, although certain studies have been carried out that the influence of *YTHDC2* on tumour promotion and suppression[33, 34]. We

investigate the m^{6}A RNA Methylation Regulators of IFN-γ with immune infiltrates in SKCM. This study aimed to access the correlations of m^{6}A RNA methylation regulators with prognosis, IFN-γ, and TIME in SKCM.

Methods

Datasets

The RNA-seq transcriptome profiles of patients with SKCM and corresponding clinical data were retrieved from the cancer genome atlas (TCGA) database (https://portal.gdc.cancer.gov/)and Gene-Expression Omnibus (GEO, GSE54467) database (https://www.ncbi.nlm.nih.gov/geo/)with R 4.0.5 software (Vienna, Austria). The 813 matched normal transcriptome data were derived from TCGA and Genotype-Tissue Expression GTEx (https://www.gtexportal.org/home/index.html) as described. The data cut-off date of SKCM samples and adjacent normal tissues was December 15, 2018. The clinical data was conducted in accordance with the International Conference. Lastly, 471 patients with SKCM and with the corresponding clinicopathological information, including age, gender and stage were enrolled for further analysis. Regarding the copy number variations (CNVs) analyses, we used TCGA data. The baseline clinicopathological features of the three cohorts are summarized in Table S1. The GEO: GSE54467 dataset from GEO database was used as the external validation cohort. The expression profiling of 270 SKCM patients and survival information were extracted from GEO. And CNV, mutation, mRNA expression data were open to the public under some guidelines.

M6a Rna Methylation Regulator Selection And Definition

According to previously published literature, 23 m^{6}A RNA methylation regulators were collected, including writers, such as *METTL3, METTL14, METTL16, RBM15, RBM15B, WTAP, ZC3H13, VIRMA*, erasers such as *FTO* and *ALKBH5*, and readers such as *YTHDC1, YTHDC2, IGF2BP1, IGF2BP2, IGF2BP3, YTHDF1, YTHDF2, YTHDF3, HNRNPA2B1, HNRNPC, RBMX, FMR1*, and *LRPPRC*. A total of 20 m^{6}A methylation regulators were identified on the basis of available mRNA expression data of SKCM from TCGA. Next, the differential expression of the 23 m^{6}A regulators was determined in the tumour tissues versus adjacent normal pairs.

Bioinformatics Analysis

TMB is calculated by the total number of mutations covered bases. We constructed a model based on the TMB status and classified SKCM into high TMB and low TMB groups by the mean of population TMB. Signatures were screened by selecting the optimal penalty parameter correlated using m^{6}A regulators. Based on the original expression data obtained from TCGA, we picked up 13 m^{6}A regulatory genes which were associated with patient survival rate and developed a risk signature using a least absolute shrinkage and selection operator (LASSO) regression model. The violin plots were drawn using R package “vioplot” to show the differential expression of 23 m^{6}A RNA methylation regulators in the tumor tissues versus adjacent normal pairs. Overall survival (OS) was calculated from the date of diagnosis to the date of death or last follow-up. And draw the heatmap through the R package “pheatmap”. To functionally elucidate the biological characteristics of the m^{6}A regulators in SKCM, we employed the “Consensus Cluster Plus” package (http://www.bioconductor.org/) to classify the patients with SKCM into different subtypes. The PCA was performed using the R package “ggplot2” to assess gene-expression patterns among distinct SKCM subtypes. Multivariate Cox regression analyzed the correlation between clinical variables and overall survival rate of SKCM patients for further evaluate the risk signature.

The GSEA was conducted in the Hallmark gene set “h.all.v6.2.symbols.gmt” of MSigDB by using the JAVA program to illustrate the difference in survival among three different SKCM subtypes. The algorithm of random sampling was 1,000 permutations. Adjusted p value < 0.05 was considered to be statistically significant. An enrichment pathway between two subtypes and the correlation between m^{6}A members was determined by Person's test. Gene ontology (GO) and Kyoto Encyclopedia of Genes and Genomes (KEGG) pathway enrichment analysis were conducted with R language “cluster Profiler” and “enrich plot” package. And the false discovery rate (FDR) < 0.05 was set as the threshold. Bar chart was used to visualize the biological process (BP), cellular component (CC) and molecular function (MF) of GO enrichment. The bar chart was also used to visualize the pathways of KEGG. The immune infiltration levels were quantified using enrichment scores calculated by single-sample gene set enrichment analysis(ssGSEA). We used the ssGSEA score to classify patients grouped by clustering subtypes and rate of survivors. The effect of the m^{6}A regulators on immune cell infiltration levels (immunoscore) was evaluated by the R package “ESTIMATE” that consisted of three immune cell types (i.e.,CD4 + T cells, eosinophilia and mast cellna) between the subgroups. The R package “CIBERSORT” (https://cibersort.stanford.edu/)was used to calculate the proportions of 24 human immune cell subsets and the fraction of immune cells types for each contained sample was yielded through cell type identification by estimating relative subsets of RNA transcripts. The algorithm of 1,000 permutations was selected.

Gene set enrichment analysis

GSEA is a computational method that performed to further realize the fundamental molecular mechanisms. In this study, we used GSEA software (Version 4.1.0) for the canonical pathway analysis based on Kyoto Encyclopedia of Genes and Genomes (KEGG) pathway, functional analysis of biological process (BP) of Gene Ontology (GO) term enrichment analysis, Reactome database analysis, and immunologic signature gene set analysis. Normalized enrichment score |NES| > 1, nominal p-value (NOM p-value) < 0.05, and a false discovery rate (FDR) q-value < 0.1 were used to sort pathways enriched in each phenotype.

Statistical analysis

All statistical tests were carried out adopting R software(version 4.0.5). And Cystoscope 4.0 was used for analysis. The differential expression levels of the m^{6}A RNA methylation regulators were compared with the Spearman correlation coefficients in cancer tissues versus normal tissues. Students test and one-way ANOVA followed by Tukey's test were used to separately perform the group comparisons of two subgroups and more than two subgroups. The correlation of clinicopathologic variables and risk signature were investigated by chi-squared test or Fisher's exact test in the validation cohorts. Overall survival was assessed using the Kaplan-Meier method, and the log-rank test was used to test for differences between the groups. Subtypes, clinicopathological features, m^{6}A scores, IFN-γ, and immune infiltration levels were summarized to correlation analysis by descriptive statistics. All 23 m^{6}A regulators of multivariate analyses were conducted Cox regression models to build a prognostic model of the independent prognostic value integrated other clinical features. Briefly, the predictive efficiency of the m^{6}A regulator-relevant signatures for 5-year OS was estimated using the curves with hazard ratios (HRs) and 95% confidence intervals (CIs). Biomarker correlations were estimated using Spearman correlation coefficients and one-sided P value. $P < 0.05$ was indicated statistically significant.

Results

Mutations and CNVs of m^{6}A RNA methylation regulators in SKCM

Among the SKCM cases with CNV (Copy number variations) data from TCGA dataset, the CNVs mutation pattern of variation frequency showed that the number of copies gained (Red) is less than the number of copies lost (Green) (Fig. 1a). In detail, the frequency of CNVs of gene *WTAP* was the highest (9.75%,46/472), that of *VIRMA* was the lowest from 23 m^{6}A regulatory genes (6.36%,30/472), which were m^{6}A "writer" genes, implying an important role of m^{6}A writer genes in SKCM. As shown in **Table 1**, a total of the CNV mutation patterns by this sequencing analysis were depended on 24 chromosomes. We also observed the circles to indicate the relationship clearly (Fig. 1b). The results also revealed that CNVs led to loss of copy number, while the outermost ring represents the human chromosomes and highlights the m^{6}A methylation regulators on this map.

Expression of m^{6}A methylation regulators and clinicopathological features in SKCM

To assess the distinct expression pattern of m^{6}A regulators in the character and function of SKCM, we scrupulously investigated the RNA expression profiles of 23 m^{6}A regulatory genes between 471 tumor samples and 273 normal skin pairs, derived from the available TCGA and GTEx datasets. The expression levels of "writers" (i.e., *ZC3H13*, *RBM15*, and *RBM15B*,), "readers" (i.e., *YTHDF1*, *YTHDF2*, *YTHDF3*, *LRPPRC*, and *IGFBP2*), and "erasers"(*ALKBH5*) were memorably higher in SKCM tissues than in normal adjacent tissues($p < 0.001$) (Fig. 2a). Furthermore, we downloaded their corresponding clinical data and incorporated 460 samples from TCGA datasets and 79 samples from GEO datasets, then assessed by Kaplan-Meier survival analysis paired with Log-rank test. The results revealed the 13 m^{6}A regulated genes were poor survivals($p < 0.05$) (Fig. 2b). To further understand the interactions among m^{6}A regulators, we found that network map showed the top 20 significant survival favorable factors and *WTAP* gene and *LRPPRC* had the strongest correlation(Fig. 2c).

Furthermore, the results of genetic expression in the TCGA database, 97/467 (20.77%)patients showed genetic alteration of m^{6}A methylation regulators. The 9 m^{6}A methylation regulators showed in **Fig. s1d.** Missense mutation was the highest mutation in the six variant classifications. *YTHDC1*,*ZC3H13*,*LRPPPRC*, *YTHDC1*, and *YTHDF1* were the most frequently altered m^{6}A methylation genes(an alteration rate of 3%). And the results of single nucleotide variants (SNVs) indicated T > A had the highest incidence in six base substitutions (C > A, C > G, C > T, T > A, T > C and T > G). The waterfall map summarized the high mutated genes and their mutation classification of SKCM(Fig. 3a). Additionally, the results indicated that the expression of *IGFBP1* gene was significant difference with *ZC3H13* wild and *ZC3H13* mutation samples($p = 0.037$)(Fig. 3b).

Significant correlation of consensus clustering for m ^{6} A RNA methylation regulators

The k = 3 was identified with optimal clustering increasing from k = 2 to 9 based on the similarity displayed by the expression levels of m^{6}A regulators and the proportion of ambiguous clustering measure(**(Figs. s1a, s1b and s1c**). A total of 471 patients with SKCM were clustered into three subtypes, namely, m^{6}Acluster.A(n = 278), cluster B(n = 199), and m^{6}Acluster.C(n = 70) (Fig. 4a). And the overall survival(OS, $p = 0.003$) in three subtypes is significant correlation(Fig. 4b). Principal component analysis(PCA) could better distinguish between patients in three clusters(Fig. 4c). On basis of correlation analysis of clinical characteristics, the expression of individual m^{6}A methylation regulator was the lowest in m^{6}Acluster.B, especially the expression levels of *IGFBP2*. Therefore, the clinicopathological features between the three subtypes were then compared in the heat map(Fig. 4d). Above this outcome we got 15 differential genes and performed the ssGSEA to conduct enrichment analysis(Fig. 4e).The results from gene ontology (GO) and Kyoto Encyclopedia of Genes and Genomes (KEGG) enrichment analysis indicated the 15 differential genes were significantly enriched in ten related pathways such as regulation of metal ion transport, and regulation of cell morphogenesis**(Figs. s2a and s2b**).

Consensus clustering of three distinct m^{6}A patterns based on the m^{6}A RNA methylation regulators associated with TIME

All m^{6}A regulators were enrolled in univariate and multivariate cox regression. Finally, 4 variables genes including *CYP2U1, SEMA6A, GRIA2*, and *TSPAN13* were selected in cox regression(**Table. 2**). We obtained m^{6}A-related genes between the three distinct m^{6}A patterns, including m6A.gene.cluster.A, B, and C**(**Fig. 5a**)**. It also depended on the proportion of ambiguous clustering measure (**Figs. s2c, s2c and s2e**). Then, we

compared these genes with m^{6}A methylation regulators. And the boxplot indicated that most m^{6}A regulators were high expression in m^{6}A.gene.cluster.C(Fig. 5b**).** And the overall survival(OS) between three subtypes was significant correlation ($p < 0.001$)(Fig. 5c**)**. Subsequently, the correlation with clinical features and four variables' genes was showed in the heat map(Fig. 5d**).**

Association of IFN-γ with m^{6}A RNA methylation in SKCM

To explore the involvement of IFN-γ with m^{6}A RNA methylation, we assessed differential expression in two subtypes and the correlation of IFN-γ with m^{6}A regulators. The expression level of IFN-γ was upregulated in SKCM tissues compared with normal adjacent tissues($p < 0.001$; Fig. 6a). Subsequently, we evaluated m^{6}A score and divided them into high and low subgroups to investigate the effect of m^{6}A regulators on the TME of SKCM. The expression level of IFN-γ in the m^{6}A score cluster was distinctly higher than that in the high m^{6}A score cluster ($p = 0.0074$; Fig. 6b). In the TCGA cohort, the expression of IFN-γ had a significantly positive association with *WTAP*, *YTHDC2, RBM15* and *FMR1* expression levels, whereas a significantly negative correlation was noted with *METTL3, METTL16,VIRMA, RBM15B, YTHDC1, YTHDF1, YTHDF2, YTHDF3, LRPPRC, HNRNPA2B1, IGFBP1, IGFBP2, IGFBP3, RBMX*, and *FTO* expression levels. Among them, IFN-γ and *WTAP* were the most positive correlation(Fig. 6c). The association of m^{6}A types and SKCM patients' prognosis was indicated by comparing survival rates of two m^{6}A score subgroups. Therefore, the OS of the low m^{6}A score were related to poor survival with expression profiles of 23 m^{6}A regulatory genes($p < 0.001$)(Fig. 6d). Subsequently, we analyzed the fraction of 23 immune cell types between the three m^{6}A clusters, which were significant difference in these immune infiltrate level. The m^{6}Acluster.B showed higher infiltration levels of Activated CD4.T.cellna, and Eosinophilia(Fig. 6e), whereas m^{6}Acluster.C was more correlated with Mast cellna. Subsequently, we inferred that there is complex correlation among m^{6}Acluster, m^{6}A.gene.cluster, m^{6}A scores, and survival state. The m^{6}A.gene.cluster.A was corresponding to high m^{6}A score, and half was alive, we drew a Sankey diagram to explore these correlations(Fig. 6f). The co-expression heat map of diversified immune cells seen in Fig. 6g. It indicated that Activated CD4.T.cellna was positively correlated with Activated CD8.T.cellna and Immature.B.cellna. Finally, we assessed the patients in m^{6}Acluster.C and m^{6}A.gene.cluster.C had higher m^{6}A score.(Figs. 6h and 6i).

Gene Set Enrichment Analysis in SKCM

In Gene Set Enrichment Analysis(GSEA), the functional meanings pathway analysis is based on the KEGG database[35]. It shows a strong significant enrichment in "Chemokine signaling pathway" when the gene set was put in order by NES(NES = 2.81, $p < 0.0001$; Fig. 7a). The following is "Fc gamma R-mediated phagocytosis"(NES = 2.74, $p < 0.0001$), "Natural killer cell mediated cytotoxicity" (NES = 2.69, $p < 0.0001$), and "Toll-like receptor signaling pathway" (NES = 2.68, $p < 0.0001$). The detail information of former 10 significantly enriched pathway are listed in Table s1. As the same based on Reactome Pathway Knowledge, we found that "Programmed Cell Death" was the most significant term(NES = 3.08, $p < 0.0001$; Fig. 7b), followed by "C-type lectin receptors" (NES = 3.07, $p < 0.0001$), "Dectin-1 signaling"(NES = 3.03, $p < 0.0001$), "Signaling by Interleukins" (NES = 2.95, $p < 0.0001$). Other details are listed in Table s2.

The biological process ontology analysis subset of gene ontology(BP subset of GO analysis) in GSEA also showed enrichment of gene sets involved in "GOBP activation of innate immune response" (NES = 3.07, $p < 0.0001$; Fig. 7c), "GOBP innate immune response activating signal transduction" (NES = 2.99, $p < 0.0001$), and "GOBP response to interleukin 12"(NES = 2.98, $p < 0.0001$). The other details are listed in Table s3.

In addition, GSEA revealed immunologic signature gene sets "GSE19941 IL10 KO vs. IL10 KO and NFKBP50 KO LPS STIM macrophage DN"(NES = 3.29, $p < 0.0001$; Fig. 7d), "GSE12845 IGD NEG blood vs. naïve tonsil bcell UP" (NES = 3.26, $p < 0.0001$), and"GSE25088 ROSIGLITAZONE vs. IL4 and ROSIGLITAZONE STIM STAT6 KO MACROPHAGE DAY10 DN" (NES = 3.21, $p < 0.0001$). Other information are summarized in Table s4.

Other clinicopathological features and TMB outcome by m^{6}A score

The OS was obtained when TMB was dichotomized at intermediate to high versus low, and the survival differences were statistically significant($p < 0.001$, Fig. 8a). Then, we depend on the m^{6}A score cluster was significant($p < 0.001$, Fig. 8b). Hence, the mutational landscapes. *TTN* gene is the most in high- m^{6}A score and low-m^{6}A score (Figs. 8c and 8d). High- m^{6}A score in alive is 58%, and low- m^{6}A score in alive is 40%. The survival state including alive and dead were obvious differences($p = 0.029$, **Figs. s4a and s4b**). Other clinicopathological features such as stage and age, we complain 1-($p = 0.003$), 3–4($p < 0.001$)and > 60, <=60(**Figs. s4c and s4d**) in the next.

Discussion

Skin is a complex organ covering the largest surface of human beings and is a common site of cancer in humans. Melanocytes are known as a kind of widely distributed and situated above skin cells[36]. And the patients of SKCM in clinical practice have poor prognosis and unsatisfactory effect. In the lasted survey, the morbidity and mortality rates of the disease differ widely across the worldwide depending on access to early detection and primary care. With the development of drug therapy and targeted therapy, the 5-year survival rate of patients has improved a lot, but local recurrence and drug sensibility still existed in SKCM treatment[37]. The m^{6}A methylation is the most abundant internal modification of RNA in post-transcriptional regulation, and affects biological functions of RNA expression and RNA-protein interactions of various tumors progression. Since more studies have focused on the mechanisms and biomarkers of malignancies, further studies focusing on m^{6}A regulators is approves to illustrate the potential immunotherapies of m^{6}A methylation in TIME. Klein et al. highlight the predictive value of tumor infiltrating lymphocyte clusters in malignant

melanomas, which is a potential biomarker[38]. Therefore, more therapeutic targets and regulatory mechanism of m^6A regulators on the TIME of SKCM must be identified.

In our study, we demonstrated the expression patterns, prognostic values, and effects on the TIME of m^6A regulators in SKCM. We probe into the mutation pattern of variation frequency on 24 human chromosomes. The frequency of CNVs of gene WTAP was the highest from m^6A regulators. And the VIRMA was the lowest from 23 m^6A regulatory genes. In contrast, the expression of were positively correlated with six immune cell infiltrations Activated CD4.T.cellna, CD8.T.cellna and Immature.B.cellna. Yan K, et al. proposed a Cox proportional hazards regression model of melanoma M2 macrophages for generating prognosis score in patients[39]. On that basis, CD8 + T cell-related factors and the co-expression network in melanoma. They identified nine-gene signature as immune checkpoint inhibitors[40, 41]Similarly, the recombination of m^6A regulators on chromosomes is similar. Lee JH, et al elucidated a novel role of mark m^6A in control of the chromosomal reorganization in cancer cells[42]. Based on these locations probabilities to understand the importance of genes is easier.

Our results showed that WTAP gene and LRPPRC had strong correlation with each other, which were significantly survival favorable factors. The WTAP also plays a carcinogenic role through activating signaling pathways[43]. WTAP regulates m^6A modification via m^6A dot blot experiment[44]. The expression of YTHDC1 is significant between SKCM and normal skin. Clinicopathological features of SKCM is divided those transcriptome datasets into high- and low-risk groups in TCGA, GTEx and GEO cohorts. To the mutated of mutation classification that the expression of IGFBP1 gene was significant difference with ZC3H13 wild and ZC3H13 mutation samples. Emerging evidence implies that m^6A modification is tightly associated with proto-oncogene activation and cancers development[22, 44, 45]. The YTHDC1 increased translation in an m^6A-dependent manner by binding to m^6A-modified mRNA, while promoting the overall translation output. Thereby of ovarian cancer is promoting the occurrence and metastasis[46–48].

However, there still remains numerous challenges in m^6A RNA methylation research recently. Divide these m^6A regulators into three clusters with clinical characteristics through principle component analysis. It is worth nothing that our results also identified significant differences among SKCM subgroups with poor survival. Li Y, et al. filtered the immune-associated 12 DEGs, six of these genes with independent prognostic[37, 49, 50]. In our study, there are four of m^6A RNA methylation regulatory factors, including CYP2U1, SEMA6A, GRIA2, and TSPAN13.

We explore the potential tumorigenesis mechanism of IFN-γ with TIME. The former scholars were investigated about anti-PD-1 resistance and occurrence of melanoma[51–53]. Hänze J, et al. showed that high PD-L1-mRNA levels in tumor tissues with a positive IFN-γ signature favorably affect OS[41, 54, 55]. These findings suggest that FTO may promoting this immunology process in tumors immune treatment which have a favorable prospect of treatment and investigation. The ssGSEA results indicated that the malignant functional features of the tumor were significantly enriched in the cluster.C with high m^6A score. Taken together, IFN-γ plays a crucial role in regulating the progression of SKCM through modulation of chemokine signaling pathway rather than a single pathway. Therefore, more studies are expected to deeply depict the function of IFN-γ in SKCM.

Conclusions

In summary, our study analyzed the m^6A RNA methylation-related genes with immune infiltrates in SKCM. These results might provide promising targets for improving the responsiveness of SKCM to immunotherapy process. We found regulator-based signatures with the immune cell infiltration levels of patients, find a novel therapeutic target based on IFN-γ. Our study provides immune pathways for further investigation into the process of m^6A regulators and its related function in SKCM.

List Of Abbreviations

m^6A - N^6-methyl adenosine

IFN-γ - Interferon -γ

SKCM - Human Skin Cutaneous Melanoma

Declarations

Orcid

https://orcid.org/0000-0002-2704-6792

Ethics approval and consent to participate

The current research was ratified by the Jilin Provincial Key Laboratory of Plant Resource Science and Green Production, Jilin Normal University.

Consent for publication

Not applicable.

Availability of data and materials

The datasets analyzed during the current study are available in the cancer genome atlas (TCGA) database (https://portal.gdc.cancer.gov/), the Gene-Expression Omnibus (GEO, GSE54467) database (https://www.ncbi.nlm.nih.gov/geo/)with R 4.0.5 software (Vienna, Austria) and Genotype-Tissue Expression (GTEx) (https://www.gtexportal.org/home/index.html).

Competing interests

The authors declare no competing interests.

Funding

This work was financially supported by the National Natural Science Foundation of China (Grant no. 31540035, 61308095, and 21801092), the program for the development of science and technology of Jilin province (Item no. 20180520002JH),

and the Thirteenth Five–Year Program for Science and Technology of Education Department of Jilin Province (Item no. JJKH20180769KJ and JJKH20180778KJ).

Authors' contributions

Methodology, Y-QW, Y-FQ, M-XL, L-H; writing, review and editing, Y-QW, Y-FQ, M-XL, L-H. All authors read and approved the final manuscript.

Acknowledgements

Thanks for the support from the National Natural Science Foundation of

China (Grant no. 31540035, 61308095, and 21801092), the program for the

development of science and technology of Jilin province (Item no. 20180520002JH),

and the Thirteenth Five–Year Program for Science and Technology of Education

Department of Jilin Province (Item no. JJKH20180769KJ and JJKH20180778KJ).

Author information

[1] Jilin Provincial Key Laboratory of Plant Resource Science and Green Production. Jilin Normal University, Siping, China;

References

1. Wei D. A multigene support vector machine predictor for metastasis of cutaneous melanoma. Mol Med Rep. 2018;17(2):2907–14.
2. Wang P, Hu L, Fu G, Lu J, Zheng Y, Li Y, Jia L. LncRNA MALAT1 Promotes the Proliferation, Migration, and Invasion of Melanoma Cells by Downregulating miR-23a. Cancer Manag Res. 2020;12:6553–62.
3. Longvert C, Saiag P. [Melanoma update]. Rev Med Interne. 2019;40(3):178–83.
4. Schadendorf D, van Akkooi ACJ, Berking C, Griewank KG, Gutzmer R, Hauschild A, Stang A, Roesch A, Ugurel S. Melanoma. Lancet. 2018;392(10151):971–84.
5. Seth R, Messersmith H, Kaur V, Kirkwood JM, Kudchadkar R, McQuade JL, Provenzano A, Swami U, Weber J, Alluri KC, et al. Systemic Therapy for Melanoma: ASCO Guideline. J Clin Oncol. 2020;38(33):3947–70.
6. Pulte D, Weberpals J, Jansen L, Brenner H: **Changes in population-level survival for advanced solid malignancies with new treatment options in the second decade of the 21st century**. *Cancer* 2019, **125**(15):2656–2665.
7. Zhou P, Wu M, Ye C, Xu Q, Wang L. Meclofenamic acid promotes cisplatin-induced acute kidney injury by inhibiting fat mass and obesity-associated protein-mediated m(6)A abrogation in RNA. J Biol Chem. 2019;294(45):16908–17.
8. Xu S, Tang L, Dai G, Luo C, Liu Z. Expression of m6A Regulators Correlated With Immune Microenvironment Predicts Therapeutic Efficacy and Prognosis in Gliomas. Front Cell Dev Biol. 2020;8:594112.
9. He L, Li H, Wu A, Peng Y, Shu G, Yin G. Functions of N6-methyladenosine and its role in cancer. Mol Cancer. 2019;18(1):176.
10. Nguyen T, Kuo C, Nicholl MB, Sim MS, Turner RR, Morton DL, Hoon DS. Downregulation of microRNA-29c is associated with hypermethylation of tumor-related genes and disease outcome in cutaneous melanoma. Epigenetics. 2011;6(3):388–94.
11. Shi H, Wei J, He C. Where, When, and How: Context-Dependent Functions of RNA Methylation Writers, Readers, and Erasers. Mol Cell. 2019;74(4):640–50.
12. Yang Y, Hsu PJ, Chen YS, Yang YG. Dynamic transcriptomic m(6)A decoration: writers, erasers, readers and functions in RNA metabolism. Cell Res. 2018;28(6):616–24.

13. Clancy MJ, Shambaugh ME, Timpte CS, Bokar JA. Induction of sporulation in Saccharomyces cerevisiae leads to the formation of N6-methyladenosine in mRNA: a potential mechanism for the activity of the IME4 gene. Nucleic Acids Res. 2002;30(20):4509–18.
14. Schwartz S, Mumbach MR, Jovanovic M, Wang T, Maciag K, Bushkin GG, Mertins P, Ter-Ovanesyan D, Habib N, Cacchiarelli D, et al. Perturbation of m6A writers reveals two distinct classes of mRNA methylation at internal and 5' sites. Cell Rep. 2014;8(1):284–96.
15. Liu J, Yue Y, Han D, Wang X, Fu Y, Zhang L, Jia G, Yu M, Lu Z, Deng X, et al. A METTL3-METTL14 complex mediates mammalian nuclear RNA N6-adenosine methylation. Nat Chem Biol. 2014;10(2):93–5.
16. Schöller E, Weichmann F, Treiber T, Ringle S, Treiber N, Flatley A, Feederle R, Bruckmann A, Meister G. Interactions, localization, and phosphorylation of the m(6)A generating METTL3-METTL14-WTAP complex. Rna. 2018;24(4):499–512.
17. Ping XL, Sun BF, Wang L, Xiao W, Yang X, Wang WJ, Adhikari S, Shi Y, Lv Y, Chen YS, et al. Mammalian WTAP is a regulatory subunit of the RNA N6-methyladenosine methyltransferase. Cell Res. 2014;24(2):177–89.
18. Qi Z, Li J, Li M, Du X, Zhang L, Wang S, Xu B, Liu W, Xu Z, Deng Y. **The Essential Role of Epigenetic Modifications in Neurodegenerative Diseases with Dyskinesia**. *Cell Mol Neurobiol* 2021.
19. Garcias Morales D, Reyes JL. A birds'-eye view of the activity and specificity of the mRNA m(6) A methyltransferase complex. Wiley Interdiscip Rev RNA. 2021;12(1):e1618.
20. Barros-Silva D, Lobo J, Guimarães-Teixeira C, Carneiro I, Oliveira J, Martens-Uzunova ES, Henrique R, Jerónimo C. **VIRMA-Dependent N6-Methyladenosine Modifications Regulate the Expression of Long Non-Coding RNAs CCAT1 and CCAT2 in Prostate Cancer**. *Cancers (Basel)* 2020, 12(4).
21. Meng Y, Zhang Q, Wang K, Zhang X, Yang R, Bi K, Chen W, Diao H. RBM15-mediated N6-methyladenosine modification affects COVID-19 severity by regulating the expression of multitarget genes. Cell Death Dis. 2021;12(8):732.
22. Paramasivam A, George R, Priyadharsini JV. Genomic and transcriptomic alterations in m6A regulatory genes are associated with tumorigenesis and poor prognosis in head and neck squamous cell carcinoma. Am J Cancer Res. 2021;11(7):3688–97.
23. Li X, Xie X, Gu Y, Zhang J, Song J, Cheng X, Gao Y, Ai Y. **Fat mass and obesity-associated protein regulates tumorigenesis of arecoline-promoted human oral carcinoma**. *Cancer Med* 2021.
24. Han T, Xu D, Zhu J, Li J, Liu L, Deng Y. Identification of a robust signature for clinical outcomes and immunotherapy response in gastric cancer: based on N6-methyladenosine related long noncoding RNAs. Cancer Cell Int. 2021;21(1):432.
25. Shi H, Wang X, Lu Z, Zhao BS, Ma H, Hsu PJ, Liu C, He C. YTHDF3 facilitates translation and decay of N(6)-methyladenosine-modified RNA. Cell Res. 2017;27(3):315–28.
26. Gan H, Hong L, Yang F, Liu D, Jin L, Zheng Q. [Progress in epigenetic modification of mRNA and the function of m6A modification]. Sheng Wu Gong Cheng Xue Bao. 2019;35(5):775–83.
27. Huang X, Lv D, Yang X, Li M, Zhang H. m6A RNA methylation regulators could contribute to the occurrence of chronic obstructive pulmonary disease. J Cell Mol Med. 2020;24(21):12706–15.
28. Li J, Rao B, Yang J, Liu L, Huang M, Liu X, Cui G, Li C, Han Q, Yang H, et al. Dysregulated m6A-Related Regulators Are Associated With Tumor Metastasis and Poor Prognosis in Osteosarcoma. Front Oncol. 2020;10:769.
29. Han J, Wang JZ, Yang X, Yu H, Zhou R, Lu HC, Yuan WB, Lu JC, Zhou ZJ, Lu Q, et al. METTL3 promote tumor proliferation of bladder cancer by accelerating pri-miR221/222 maturation in m6A-dependent manner. Mol Cancer. 2019;18(1):110.
30. Wang T, Kong S, Tao M, Ju S. The potential role of RNA N6-methyladenosine in Cancer progression. Mol Cancer. 2020;19(1):88.
31. Wang L, Zhang S, Li H, Xu Y, Wu Q, Shen J, Li T, Xu Y. Quantification of m6A RNA methylation modulators pattern was a potential biomarker for prognosis and associated with tumor immune microenvironment of pancreatic adenocarcinoma. BMC Cancer. 2021;21(1):876.
32. Wu X, Xiao Y, Ma J, Wang A. Circular RNA: A novel potential biomarker for skin diseases. Pharmacol Res. 2020;158:104841.
33. Zhang C, Guo C, Li Y, Ouyang L, Zhao Q, Liu K. **The role of YTH domain containing 2 in epigenetic modification and immune infiltration of pan-cancer**. *J Cell Mol Med* 2021.
34. Romanowska K, Rawłuszko-Wieczorek AA, Marczak Ł, Kosińska A, Suchorska WM, Golusiński W. **The m(6)A RNA Modification Quantity and mRNA Expression Level of RNA Methylation-Related Genes in Head and Neck Squamous Cell Carcinoma Cell Lines and Patients**. *Biomolecules* 2021, 11(6).
35. Kanehisa M, Furumichi M, Tanabe M, Sato Y, Morishima K. KEGG: new perspectives on genomes, pathways, diseases and drugs. Nucleic Acids Res. 2017;45(D1):D353-d361.
36. Talty R, Bosenberg M. **The Role of Ferroptosis in Melanoma**. *Pigment Cell Melanoma Res* 2021.
37. Li Y, Lyu S, Gao Z, Zha W, Wang P, Shan Y, He J, Huang S. Identification of Potential Prognostic Biomarkers Associated With Cancerometastasis in Skin Cutaneous Melanoma. Front Genet. 2021;12:687979.
38. Klein S, Mauch C, Brinker K, Noh KW, Knez S, Büttner R, Quaas A, Helbig D. Tumor infiltrating lymphocyte clusters are associated with response to immune checkpoint inhibition in BRAF V600(E/K) mutated malignant melanomas. Sci Rep. 2021;11(1):1834.
39. Yan K, Wang Y, Lu Y, Yan Z. Coexpressed Genes That Promote the Infiltration of M2 Macrophages in Melanoma Can Evaluate the Prognosis and Immunotherapy Outcome. J Immunol Res. 2021;2021:6664791.

40. Yan K, Lu Y, Yan Z, Wang Y. 9-Gene Signature Correlated With CD8(+) T Cell Infiltration Activated by IFN-γ: A Biomarker of Immune Checkpoint Therapy Response in Melanoma. Front Immunol. 2021;12:622563.
41. Hänze J, Wegner M, Noessner E, Hofmann R, Hegele A. Co-Regulation of Immune Checkpoint PD-L1 with Interferon-Gamma Signaling is Associated with a Survival Benefit in Renal Cell Cancer. Target Oncol. 2020;15(3):377–90.
42. Lee JH, Hong J, Zhang Z, de la Peña Avalos B, Proietti CJ, Deamicis AR, Guzmán GP, Lam HM, Garcia J, Roudier MP, et al: **Regulation of telomere homeostasis and genomic stability in cancer by N (6)-adenosine methylation (m(6)A)**. *Sci Adv* 2021, **7**(31).
43. Deng J, Zhang J, Ye Y, Liu K, Zeng L, Huang J, Pan L, Li M, Bai R, Zhuang L, et al: **N6-methyladenosine-mediated upregulation of WTAPP1 promotes WTAP translation and Wnt signaling to facilitate pancreatic cancer progression**. *Cancer Res* 2021.
44. Ying Y, Ma X, Fang J, Chen S, Wang W, Li J, Xie H, Wu J, Xie B, Liu B, et al. EGR2-mediated regulation of m(6)A reader IGF2BP proteins drive RCC tumorigenesis and metastasis via enhancing S1PR3 mRNA stabilization. Cell Death Dis. 2021;12(8):750.
45. Song Y, Zheng C, Tao Y, Huang R, Zhang Q. N6-Methyladenosine Regulators Are Involved in the Progression of and Have Clinical Impact on Breast Cancer. Med Sci Monit. 2021;27:e929615.
46. Zheng J, Guo J, Cao B, Zhou Y, Tong J. Identification and validation of lncRNAs involved in m6A regulation for patients with ovarian cancer. Cancer Cell Int. 2021;21(1):363.
47. Zhang C, Liu J, Guo H, Hong D, Ji J, Zhang Q, Guan Q, Ren Q. m6A RNA methylation regulators were associated with the malignancy and prognosis of ovarian cancer. Bioengineered. 2021;12(1):3159–76.
48. Wei Q, Yang D, Liu X, Zhao H, Yang Y, Xu J, Liu T, Yi P. Exploration of the Role of m(6) A RNA Methylation Regulators in Malignant Progression and Clinical Prognosis of Ovarian Cancer. Front Genet. 2021;12:650554.
49. Ju A, Tang J, Chen S, Fu Y, Luo Y. Pyroptosis-Related Gene Signatures Can Robustly Diagnose Skin Cutaneous Melanoma and Predict the Prognosis. Front Oncol. 2021;11:709077.
50. Tian Q, Gao H, Zhao W, Zhou Y, Yang J. **Development and validation of an immune gene set-based prognostic signature in cutaneous melanoma**. *Future Oncol* 2021.
51. Wu X, Wang X, Zhao Y, Li K, Yu B, Zhang J. Granzyme family acts as a predict biomarker in cutaneous melanoma and indicates more benefit from anti-PD-1 immunotherapy. Int J Med Sci. 2021;18(7):1657–69.
52. Dong X, Song J, Chen B, Qi Y, Jiang W, Li H, Zheng D, Wang Y, Zhang X, Liu H. Exploration of the Prognostic and Immunotherapeutic Value of B and T Lymphocyte Attenuator in Skin Cutaneous Melanoma. Front Oncol. 2020;10:592811.
53. Zhang Z, Li L, Li M, Wang X. The SARS-CoV-2 host cell receptor ACE2 correlates positively with immunotherapy response and is a potential protective factor for cancer progression. Comput Struct Biotechnol J. 2020;18:2438–44.
54. Kursunel MA, Esendagli G. The untold story of IFN-γ in cancer biology. Cytokine Growth Factor Rev. 2016;31:73–81.
55. Zhu Y, An X, Zhang X, Qiao Y, Zheng T, Li X. STING: a master regulator in the cancer-immunity cycle. Mol Cancer. 2019;18(1):152.

Tables

Table 1. The gene label of different m6A regulatory genes in SKCM (n = 539)

id	Type	Chromosome	chromStart	chromEnd	TMB	HR	HR.95L	HR.95H	pvalue	km
ALKBH5	erasers	chr17	18183078	18209954	0	1.08109	0.570361	2.049153	0.811119	0.063295159
FMR1	readers	chrX	147911951	147951125	3	0.54299	0.318692	0.92515	0.024696	0.069819269
FTO	erasers	chr16	53703963	54121941	1	1.685964	1.044856	2.720447	0.032378	0.000231246
HNRNPA2B1	readers	chr7	26189927	26201529	8	0.855033	0.601155	1.216127	0.383571	0.073341036
HNRNPC	readers	chr14	21209136	21269494	0					
IGFBP1	readers	chr7	45888357	45893668	6	0.808665	0.707638	0.924115	0.001815	0.000375161
IGFBP2	readers	chr2	216632828	216664436	4	0.980024	0.852582	1.126517	0.776496	0.237473672
IGFBP3	readers	chr7	45912245	45921874	4	0.843073	0.688059	1.03301	0.099624	0.049129068
LRPPRC	readers	chr2	43886508	43996005	13	1.232921	0.746293	2.03686	0.41366	0.033402751
METTL14	writers	chr4	118685368	118715433	16					
METTL16	writers	chr17	2405562	2511891	8	1.485847	0.888776	2.484026	0.130976	0.000589839
METTL3	writers	chr14	21498133	21511375	3	0.809072	0.501574	1.305087	0.385132	0.01842991
RBM15	writers	chr1	110338506	110346681	5	1.07707	0.653046	1.776414	0.771182	0.031130036
RBM15B	writers	chr3	51391268	51397908	4	2.465481	1.104362	5.504171	0.02765	6.80E-05
RBMX	readers	chrX	136848004	136880764	6	0.796724	0.5057	1.255227	0.327169	0.012244959
VIRMA	writers	chr8	94487693	94553529	0	0.88507	0.513128	1.526616	0.6607	0.203700173
WTAP	writers	chr6	159725585	159756319	3	0.445755	0.259969	0.764313	0.003315	3.13E-05
YTHDC1	readers	chr4	68310387	68350089	16	0.663254	0.331206	1.328194	0.2465	0.094602479
YTHDC2	readers	chr5	113513683	113595285	13	0.809507	0.541048	1.211172	0.303951	0.001471831
YTHDF1	readers	chr20	63195429	63216234	13	1.939769	0.978418	3.845701	0.057765	0.002425318
YTHDF2	readers	chr1	28736621	28769775	5	0.996907	0.621323	1.599528	0.989754	0.161101116
YTHDF3	readers	chr8	63168553	63212786	6	1.050144	0.636696	1.732071	0.848023	0.010144971
ZC3H13	writers	chr13	45954465	46052759	14					

Table 2. The four genes with overall survival data

Gene	HR	HR.95L	HR.95H	P value
CYP2U1	1.332446	1.063148	1.669957	0.01272
SEMA6A	1.39865	1.205885	1.62223	9.24E-06
GRIA2	0.878746	0.804383	0.959984	0.004167
TSPAN13	0.808524	0.678494	0.963472	0.017505

Figures

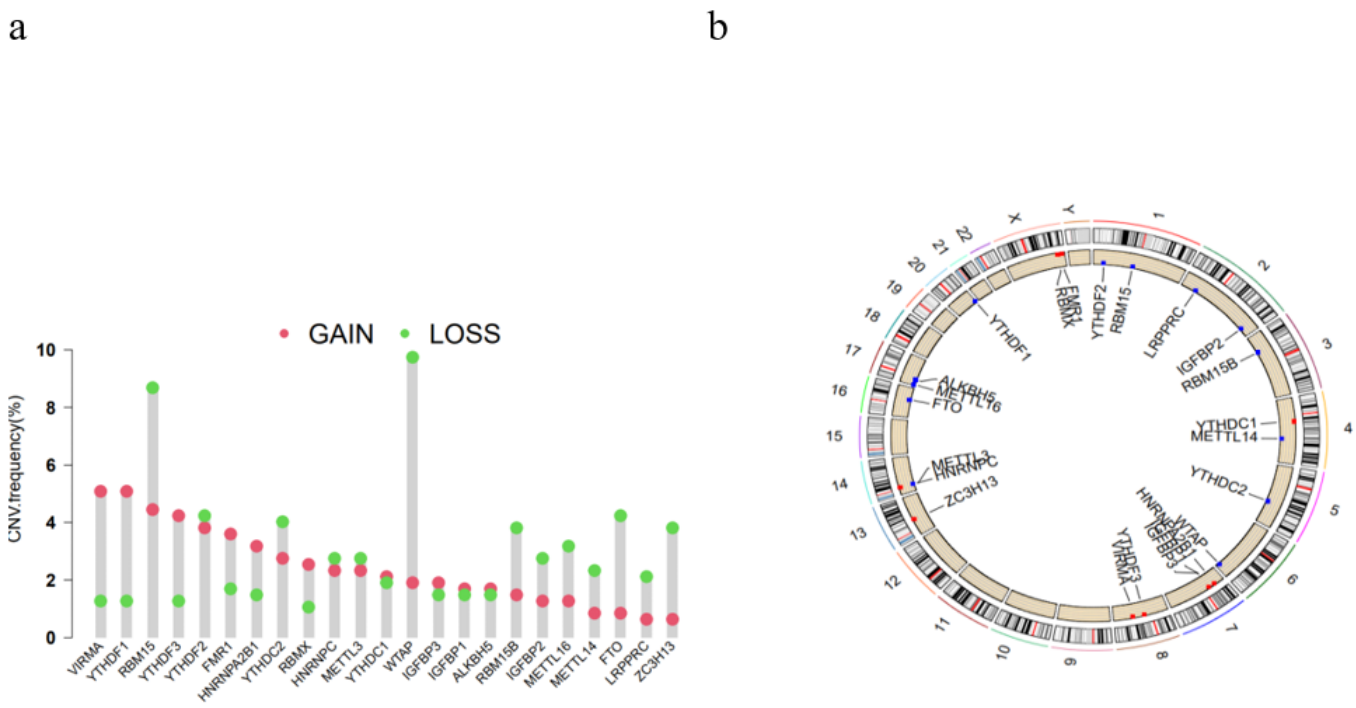

Figure 1

CNVs of m6A regulatory genes in SKCM. (a) Frequency of Skin Cutaneous Melanoma samples with CNVs in m6A regulatory factors in TCGA dataset. (b)Circle plot of differential CNVs of m6A regulatory factors on 23 chromosomes. The black dot in the outer ring indicates amplification, while the red dot in the inner ring indicates deletion.

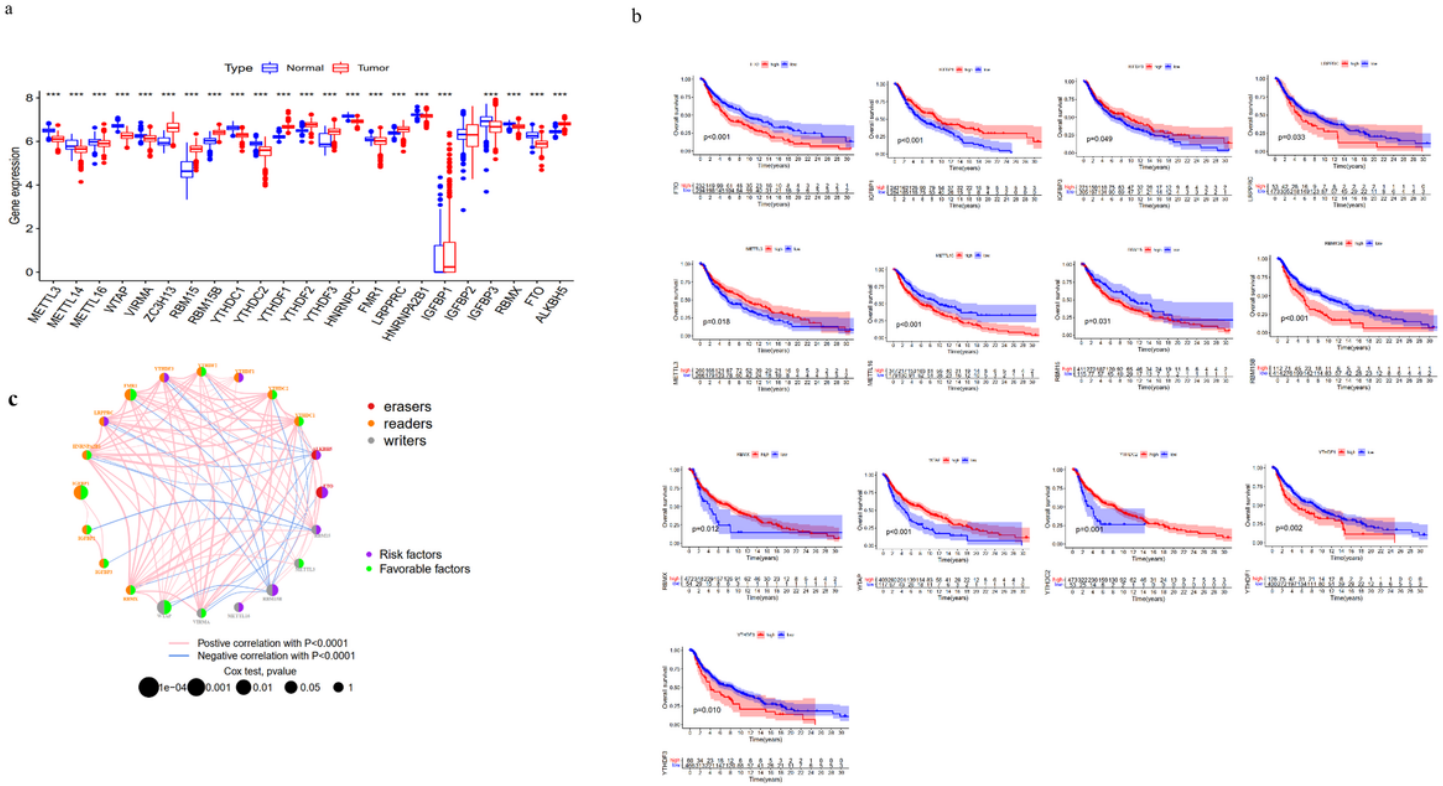

Figure 2

Expression of m6A RNA methylation reg orators and overall survival (OS) rates in SKCM. (a)The boxplot diagram revealed median expression of 23 m6A RNA regulators in tumor and normal control samples. *p <0.05, **p < 0.01, and ***p < 0.001. (b)Kaplan-Meier(K-M) curves showing the OS of

SKCM patients with low and high m6A factors. (c) A prognostic network map about positive correlation with P<0.0001. The size and color of the node denotes the degree values, respectively. Top genes with lighter colors and larger circles show higher degree value in the network.

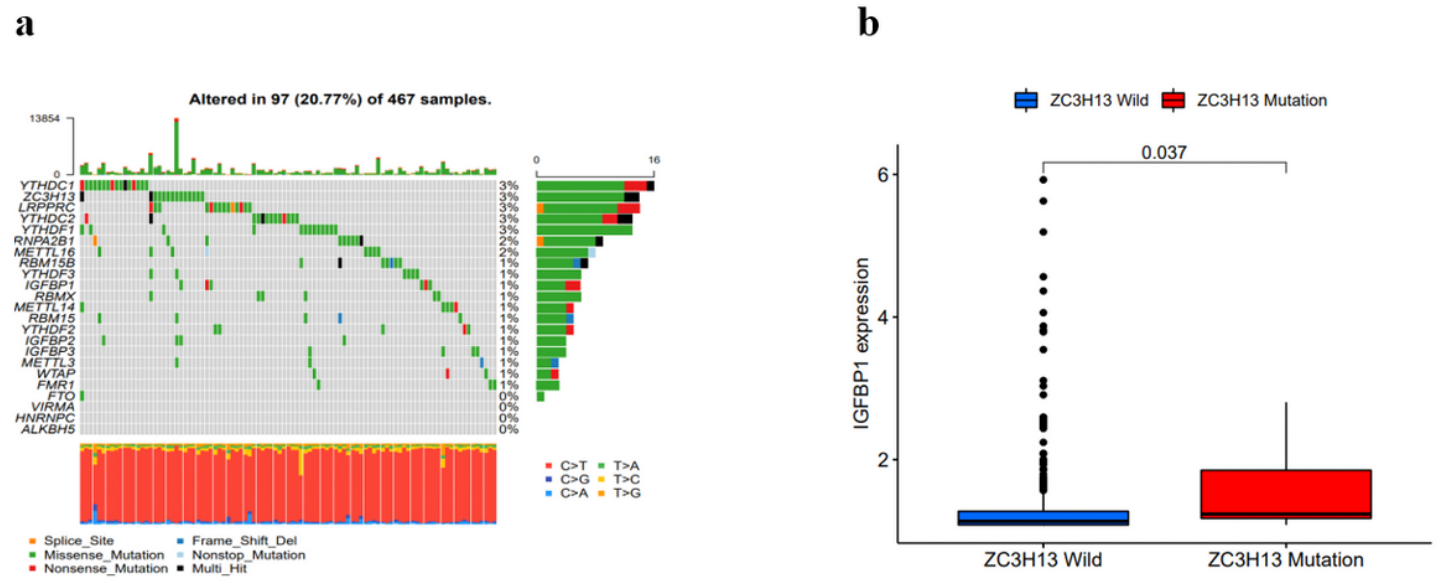

Figure 3

Summary of the tumor mutational burden (TMB) in SKCM patients. (a)The waterfall plot showed the mutation characteristics of each m6A gene in each sample and the various colors represented the different mutation types. The bar plot above the legend exhibited the mutational burden. (b) The lines in the boxes represented median value, and black dots showed outliers in ZC3H13 wild and ZC3H13 mutation samples (P=0.037).

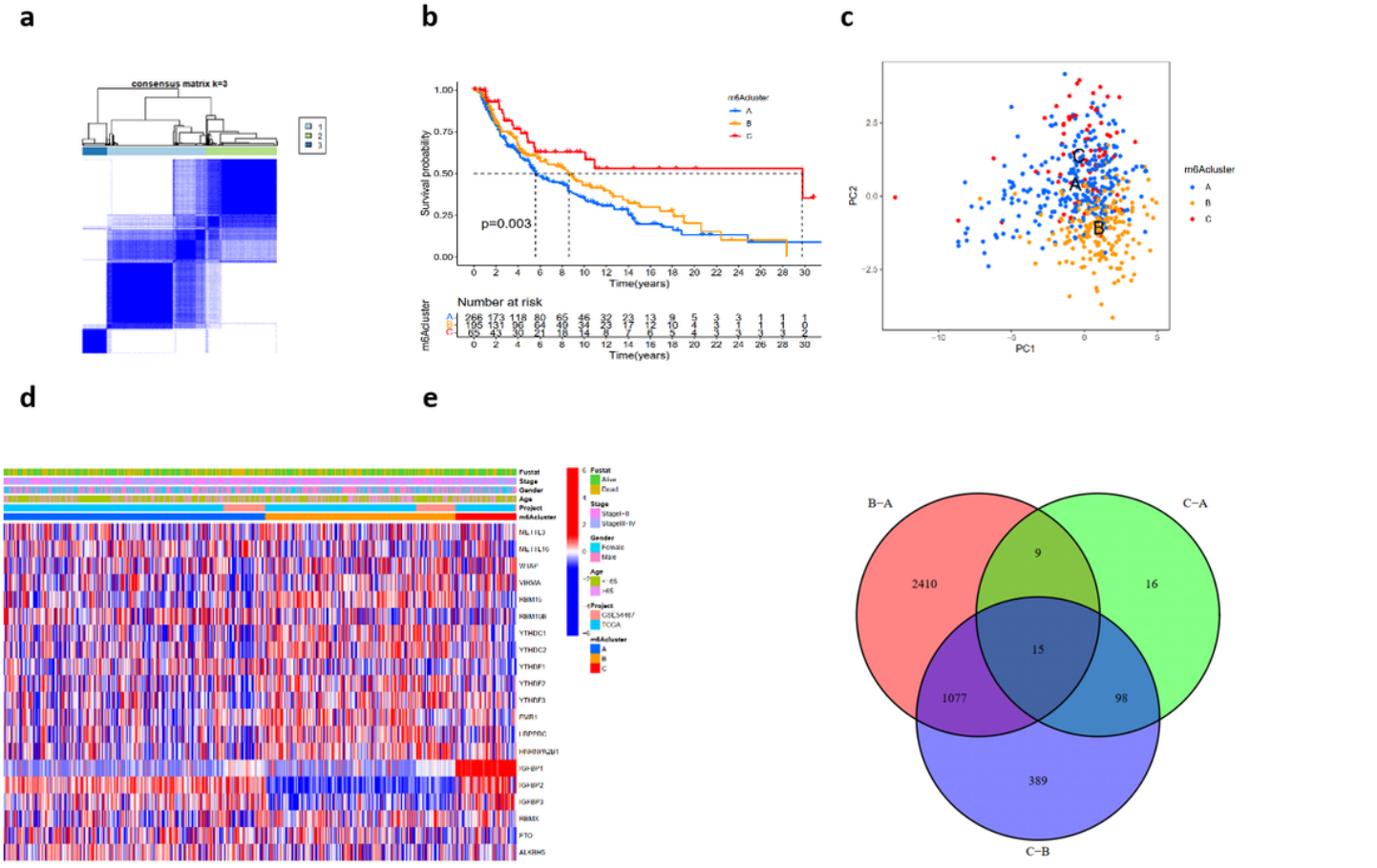

Figure 4

Differential clinicopathological features and unsupervised clustering of 20 m6A regulators in the TCGA cohort. (a) Color-coded heatmap corresponding to the consensus clustering matrix for k=3. Color gradients represent consensus values from 0 to 1. (b) Kaplan-Meier curves of OS for patients with SKCM in three m6Aclusters. (c) Principal component analysis was performed on basis of cluster analysis, showing a remarkable difference in transcriptomes between the 3 m6A patterns. (d)The heat map visualized differentially expression levels clinicopathologic features of the three m6Acluster. (e)15 DEGs were generated by comparing m6A cluster (B vs A, C vs A, C vs B).

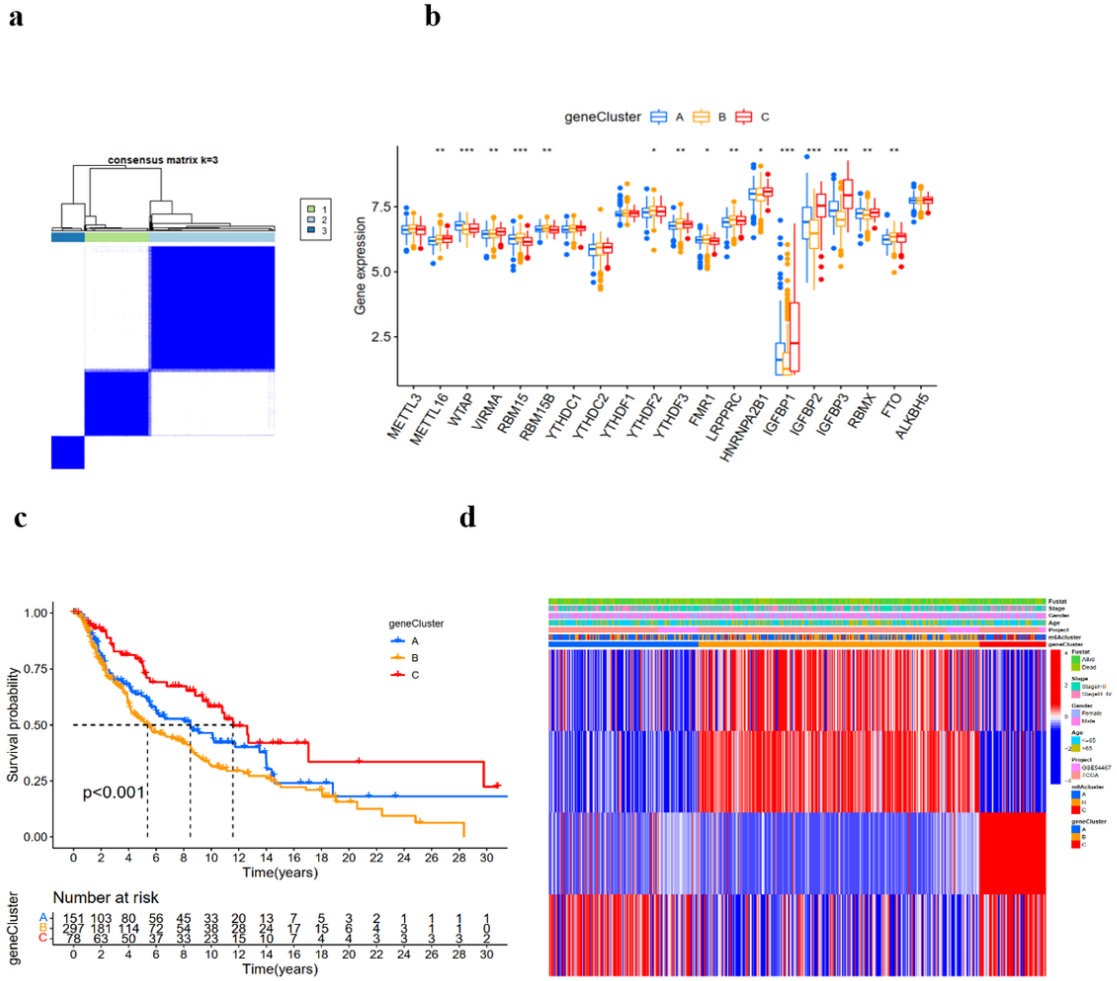

Figure 5

Consensus matrices consequences of the 20 m6A regulators. (a)Consensus matrices of the 20 m6A regulators for k=3.(b)Differential expression boxplot of the 20 m6A regulators in m6Acluster.A, m6A.gene.cluster.B and m6Acluster.C. (c)Kaplan-Meier curves showing the prognostic value of the three m6A patterns in TCGA-SKCM dataset (**P < 0.01 and ***P < 0.001). (d)The heat map showed the different expression of m6A RNA methylation regulators and the distribution of clinicopathologic features between m6A clusters and gene clusters.

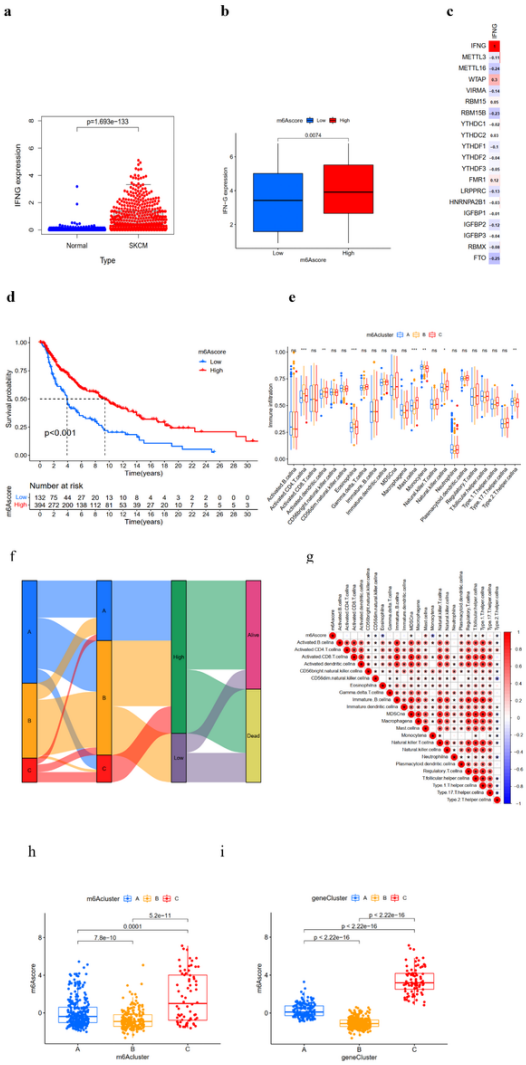

Figure 6

Association of IFN-γ with m6A RNA methylation and the landscape of clinical trial. (a) IFN-γ upregulation in SKCM in TCGA cohort. (b) The expression level of IFN-γ in high/low m6A score in TCGA cohort. (c) The correlation coefficients of IFN-γ with m6A methylation regulators obtained by Pearson correlation analysis. (d)Kaplan-Meier curves showing the prognostic value of the m6A score in TCGA-SKCM dataset. Differences in m6A score between m6A.gene.cluster.A, m6A.gene.cluster.B and m6A.gene.cluster.C (e) Immune infiltrate level between m6A score in m6A.gene.cluster.A/B/C in TCGA cohort.*p <0.05, **p < 0.01, and ***p < 0.001, ns.(f) Sankey diagram revealing the relationship between m6Acluster, m6A.gene.cluster, m6A scores, and survival state. (g) Immune correlation analysis. Differences in m6A score between m6Acluster (h) and m6A.gene.cluster (i).

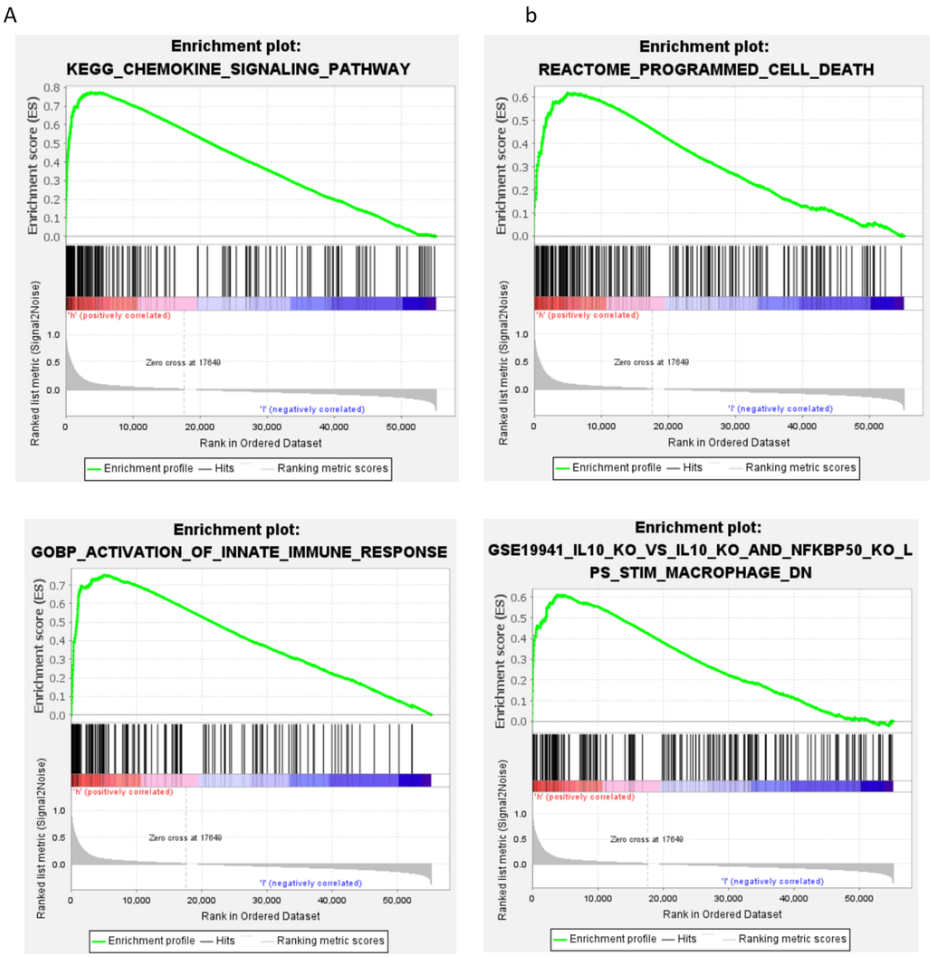

Figure 7

A Enrichment plot: (a) The most significant canonical pathwat in terms of the KEGG databases. (b) The most significant canonical pathways in terms of Reactome pathway database. (c) The most significant biological process according to Gene Ontology. (d) The most significant immunologic signature gene sets; NES = normalized enrichment score

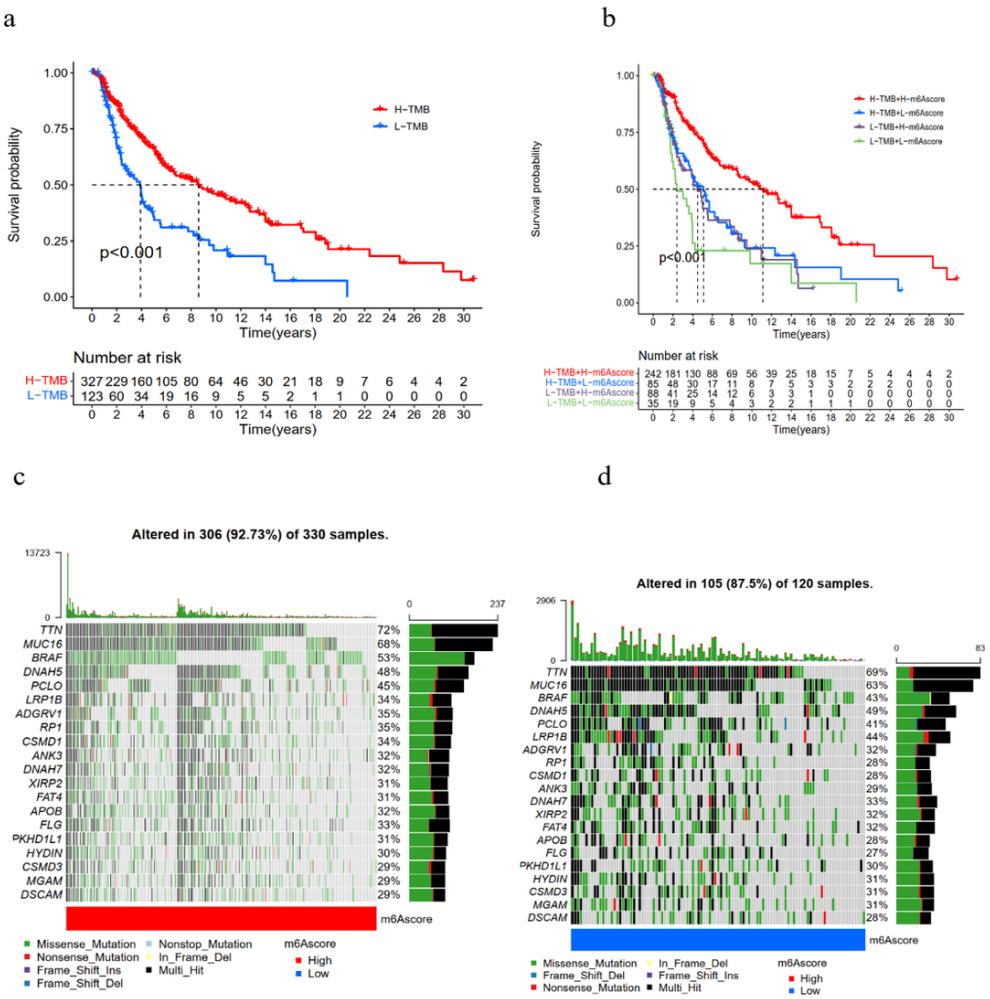

Figure 8

TMB of patients with high- and low-cluster. (a)Kaplan-Meier curves for overall survival of SKCM patients stratified by m6A-related gene set variation score (TMB) (b)Analysis of patients' data in H-TMB versus L-TMB with m6Ascore.clusters. Comparison of mutational landscapes between m6A score to high- (c)and low- score(d).

Supplementary Files

This is a list of supplementary files associated with this preprint. Click to download.

- SupplementaryMaterial.docx
- TableS1.xlsx
- TableS2.xlsx
- TableS3.xlsx
- TableS4.xlsx